24th EUROPEAN ROTORCRAFT FORUM
Marseilles, France -15th-17th September 1998

AS 03
Application of Modern Control Technology for Advanced IBC Systems

Oliver Dieterich
EUROCOPTER DEUTSCHLAND GmbH, 81663 München, Germany

Based on theoretical and experimental investigations the application of individual blade control (IBC) promises progress in the fields of vibration reduction, noise reduction, rotor stabilization, power consumption and dynamic stall delay. In order to realize the potential offered by IBC systems EUROCOPTER initiated a technology programme called RACT (rotor active control technology) aiming at the usage of advanced IBC systems with flap actuation. First milestones of the RACT programme are the implementation and the flight testing of closed loop control algorithms for simultaneous vibration and noise reduction on an experimental IBC system based on a BO105 helicopter.

EUROCOPTER has several years experience in the investigation and development of IBC. In the year 1990 first IBC flight tests were performed on a BO105 helicopter the pitch link rods being substituted by hydraulic actuators. The higher harmonic control of the IBC blade root actuators was based on open loop algorithms. In a subsequent step a corresponding main rotor equipped with IBC was tested in the 40 ft by 80 ft windtunnel at NASA Ames. The hydraulic actuators implemented for the windtunnel tests had a significantly increased authority. For the RACT programme the experimental helicopter was upgraded with improved actuators, advanced sensors, extensive measurement equipment and a fast digital computer by which the control laws are implemented. Flight tests are scheduled for 1998.

Concerning first applications of IBC systems the focus on the vibration and noise reduction tasks is a logical choice. These topics are of high importance for the industry due to the demands on modern helicopter design. Compared to HHC systems based on actuators below the swashplate IBC offers the possibility to control additional rotor modes e.g. the differential mode. This special property of IBC will be used for the simultaneous control of vibration and noise relating the differential mode to noise reduction and the remaining modes to vibration reduction. In the paper emphasis is given to the discussion of vibration reduction strategies by IBC.

A time domain approach of output vector feedback based on disturbance rejection concepts is selected for the vibration reduction part of the RACT controller. The application of the 'internal model principle' with respect to the harmonic structure of the disturbances leads to the implementation of notch filters for the vibration controller dynamics. Regarding the evaluation of the feedback gains modern procedures for the determination of optimal constant output feedback are performed with respect to linear multivariable systems. Simulations are carried out in order to demonstrate the properties of the investigated control designs.

For the controller design and realization numerical software and computer-aided control systems design (CACSD) tools are of high significance. Concerning the description of the BO105 helicopter, the results in state space form obtained by the comprehensive rotor code CAMRAD II are transferred to the CACSD system MATRIXx which serves as development environment for the vibration controller. Controller design, simulation runs, controller discretization and automatic source code generation for the digital IBC computer are integrated in the development environment as subsequent modules. Available test data are used in order to validate the design procedure. In addition, hardware components with emphasis on the vibration controller are discussed in view of hardware requirements by advanced IBC systems.

The paper demonstrates the benefits of modern control technology for the realization of future high performance IBC systems.

Notations

A, B, C, D, E, F	state space matrices	t	time
d	disturbance	u	input vector
dt	time step	x	state vector
F_x, F_y, F_z	hub forces	y	output vector
f	blade passage frequency	z	controlled disturbances
G	transfer function	z_0	uncontrolled disturbances
K_C	gain matrix	z	Z variable
k_1, k_2	gains	$\Delta\varphi$	phase shift
I	unity matrix	$\Delta\theta$	control input
i	imaginary unit	ψ_m	azimuth angle of blade m
J	quality criterion	ϑ_0	pitch angle collective mode
M_x, M_y, M_z	hub moments	ϑ_C	pitch angle longitud. mode
Q, R	weighting matrices	ϑ_S	pitch angle lateral mode
q	quality criterion	ϑ_D	pitch angle differential mode
s	Laplace variable	$\vartheta^{(m)}$	pitch angle of blade m
T	transfer matrix	ω	rotor angular velocity

1. Introduction

From theoretical point of view multicyclic control of helicopter rotors offers fascinating possibilities for the control of the lift distribution on the rotor disk. Controlling the lift distribution aims on taking influence on vibration, noise, performance and fuel consumption as well as stall delay. This technology is described as active rotor control. Individual blade control (IBC) is a special case of multicyclic control established by additional pitch control degrees of freedom for every blade. Nowadays, several hardware concepts are imaginable differing significantly in their realization states.

The most conventional concept is blade root actuation, the pitch links substituted by actuators. By extension or contraction of the actuator the pitch angle of the corresponding blade is changed without injuring the other blades of the rotor. The blade root actuation is – in some kind – comparable to higher harmonic control (HHC) systems with the distinction that the actuators are integrated in the rotating system of the rotor. IBC systems are superior to HHC systems in case of rotors with more than three blades due to additional control degrees of freedom.

A more sophisticated concept consists in the usage of rotor blade flaps, the actively controlled flaps (ACF). The deflection of a blade flap acts primarily on lift and moment variation. Regarding blade torsional flexibility the flap moments induce elastic torsion amplifying or counteracting the flap lift. According to theoretical investigations ACF has advantages in power consumption and control forces compared to blade root actuation. Due to the progress in the development of piezoelectric actuators the concept of ACF is now of high interest for realization in the near future.

During the last decade EUROCOPTER DEUTSCHLAND (ECD) made first steps towards the development of IBC systems by investigating flight tests and wind tunnel tests of the BO105 rotor system. In the years 1990 and 1991 open loop flight test campaigns were launched using a BO105 equipped with a blade root actuated IBC system. The authority of the actuators developed by ZF Luftfahrttechnik (ZFL) was limited to max. 0.42° for flight safety reasons. The investigations were mainly focused on single harmonic IBC inputs of 3/rev, 4/rev and 5/rev studying their influence on vibrations and hub loads at flight speeds of 60 KIAS and 110 KIAS. The results demonstrated a perceptible influence on cabin vibrations within the feasible control authority [1]. Nevertheless, an increase of the actuator authority seemed to be desirable for the exploration of the full potential of IBC.

In order to realize this potential, wind tunnel tests with the rotor system of the BO105 were performed in the years 1993 and 1994 in the 40 ft by 80 ft wind tunnel at NASA Ames. Actuators with increased amplitude were implemented for IBC blade root actuation. Single harmonic, multi-harmonic and wavelet IBC inputs in the frequency range of 2/rev to 6/rev and amplitudes up to 2° were applied to the IBC system [2]. One key point of the wind tunnel tests consisted in descent flight conditions characterized by the occurrence of significant blade vortex interaction (BVI) noise.

Thus, flight tests and wind tunnel tests demonstrated the effectiveness of IBC systems for vibration reduction and BVI noise reduction under selected conditions. Therefore, vibration reduction and exterior noise reduction are ideal candidates for the demonstration of benefits of IBC systems improving the acceptance of helicopters. Nevertheless, the tests showed a demand for closed loop systems for both vibration and noise control as the optimal IBC inputs are sensitive to flight parameters. Furthermore, the input for vibration minima did not necessarily correlate to the noise minima posing the question of simultaneous control for vibration and noise.

For continuation on active rotor control, ECD participates in a technology programme called RACT (Rotor Active Control Technology) [3]. One of the key points of RACT consists in the application of closed loop control for vibration and noise reduction during flight tests. Therefore, the experimental BO105 IBC system was upgraded with improved actuators and a complex electronic equipment for data processing. Control algorithms has to be developed and coded as real-time applications for the digital control computer.

In this paper the development of control algorithms with focus on vibration reduction is presented starting with theoretical considerations. Then, the evolution from theoretical work to automatically generated real-time code performed by advanced computer tools is discussed from industrial point of view. Finally an outlook to future activities is given by transferring the controller design process to the case of actively controlled flaps.

2. Controller Concepts for Noise and Vibration Control

2.1. Noise and Vibration Sources

Compared to fixed wing aircraft, fundamental differences are inherent to rotorcrafts concerning noise and vibration sources. The high noise and vibration levels are mainly based on the unsteady aerodynamic environment of the rotor blades during a revolution in forward flight. The flow pattern around the rotor blades is dominated by a global asymmetry evoked by flight velocity and angular velocity of the rotating blades. Local flow phenomena as blade vortex interactions, reverse flow, shock and stall effects are superposed to the global flow leading to significant changes of local stream conditions. If gusts and transient manoeuvres are neglected the flow pattern is of periodic structure. In Fig. 1 and Fig. 2 the periodicity of the flow pattern is demonstrated by time histories of pressure data measured at blade tip.

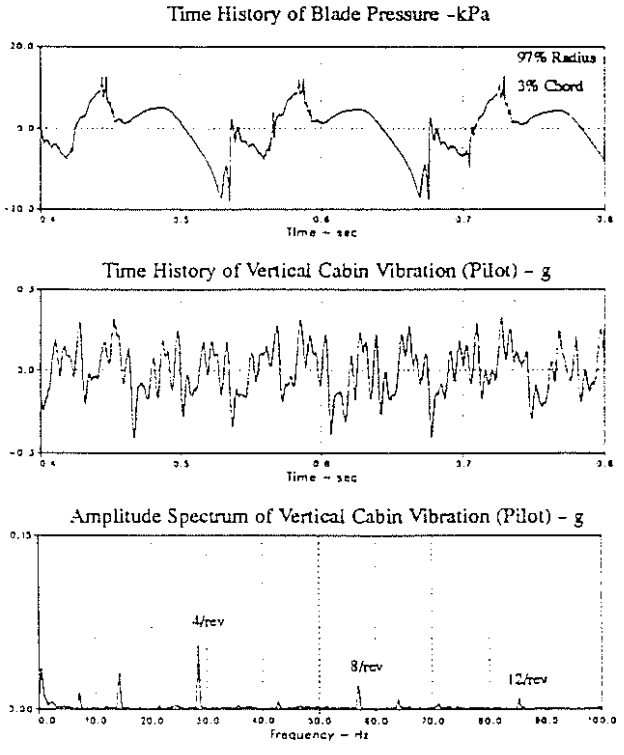

Figure 1: Typical inflight data: 6° descent at 63 kts (BO105)

In case of blade vortex interactions a pulse-type noise is generated due to the interference of a vortex structure inducing high velocities at rotor blades which pass the vicinity. This kind of noise is known as BVI noise which appears especially under descent flight conditions. In Fig. 1 the occurrence of BVI noise is visible by spikes of the pressure data. Several wind tunnel and flight tests demonstrated that BVI noise is a primary candidate for higher harmonic control [4].

As the local flow phenomena are of higher harmonic nature, the blade lift shows a broad frequency spectrum forcing the blades to adequate movements. Therefore, forces and moments acting on the hub are produced by higher harmonic aerodynamic, inertia and elastic loads of the blades. The assumptions of pure periodicity and identical blades lead to a discrete fuselage vibration spectrum based on integer multiples of the blade passage frequency, see Fig. 1 and Fig. 2. Usually the peak value is assigned to the blade passage frequency. Unfortunately, the corresponding frequency range is very sensitive for passengers demanding on special efforts for decreasing the peak.

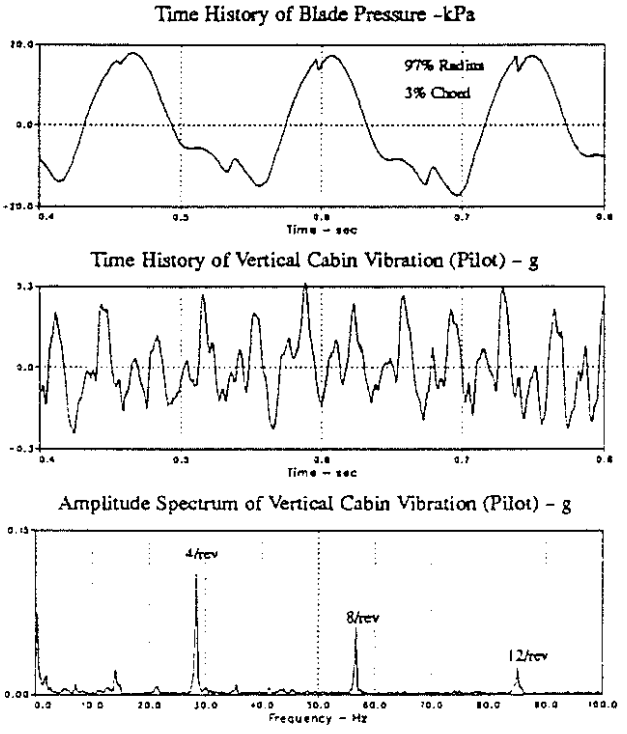

Figure 2: Typical inflight data: level flight at 110 kts (BO105)

2.2 Simultaneous Control of Noise and Vibration

Results of the NASA Ames wind tunnel tests indicated that the optimal control for BVI noise reduction may differ from optimal vibration reduction control under descendent flight conditions. Furthermore, cases exist where BVI noise reduction leads to an increase of hub load components, see Fig. 3. Therefore, advanced control concepts aiming on the simultaneous reduction of noise and vibration may have to deal with contrary targets.

For the four bladed BO105 rotor, the property of IBC systems – controlling the blade pitch angles independently – allows the usage of an additional control mode compared to pure swashplate control. In multiblade coordinates this mode is described as

differential pitch input, Fig. 4d. In order to separate noise control from vibration control a definite assignment of control modes to control task exists.

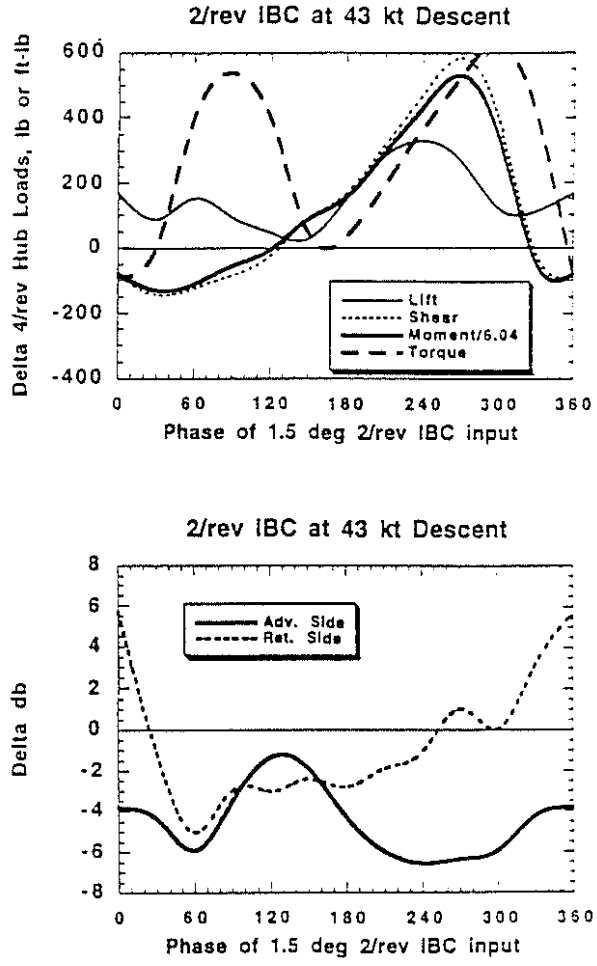

Figure 3: Noise and vibration changes due to IBC input NASA Ames wind tunnel results

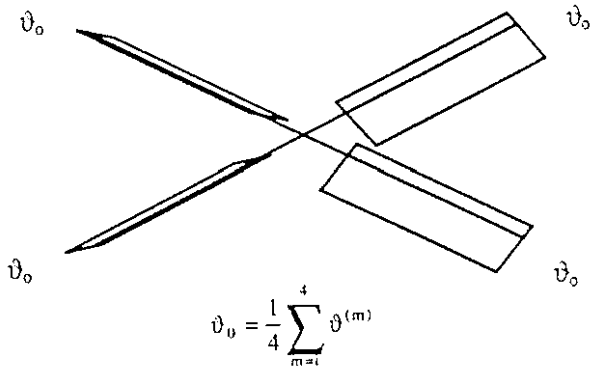

Figure 4a: Collective multiblade coordinate for a four-bladed rotor

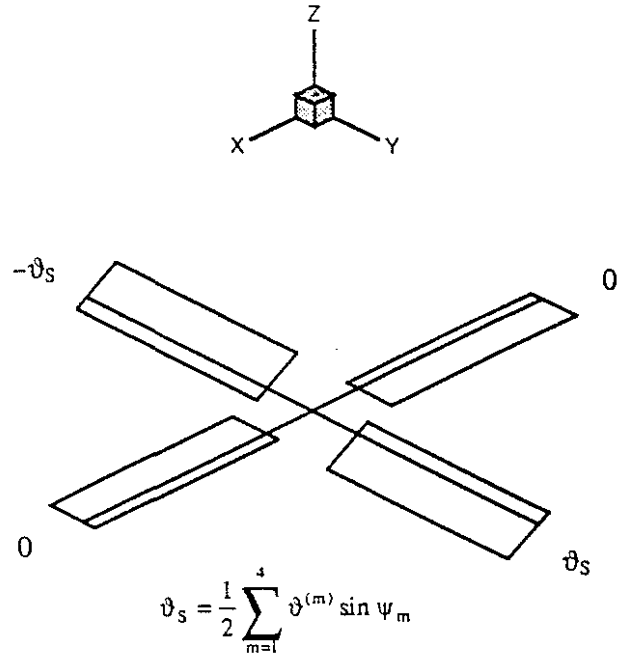

Figure 4b: Lateral multiblade coordinate for a four-bladed rotor

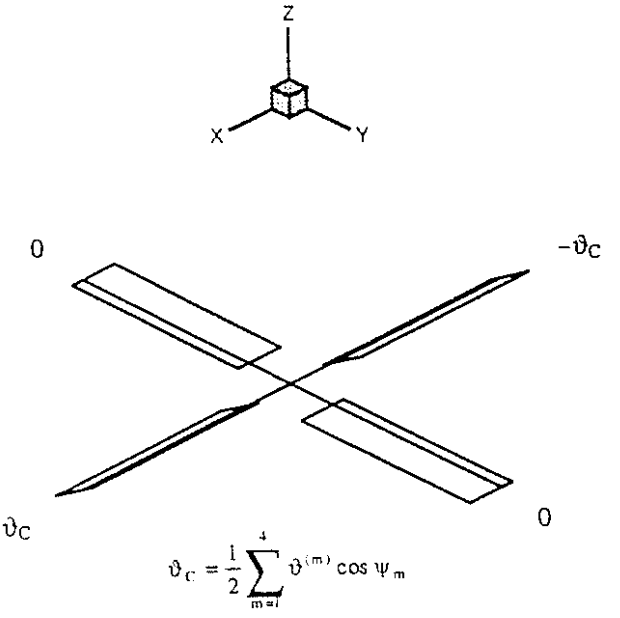

Figure 4c: Longitudinal multiblade coordinate for a four-bladed rotor

According to the wind tunnel results the differential control mode is an ideal candidate for BVI noise control as the 2/rev input mainly controls the differential mode. Vibration control is assigned to the collective, the longitudinal and the lateral control modes. Under steady conditions these control modes are excited at blade passage frequency of 4/rev by the vibration controller. If these multiblade inputs are transformed to individual blade inputs the pitch frequency of the blades is spread to 3/rev, 4/rev and 5/rev.

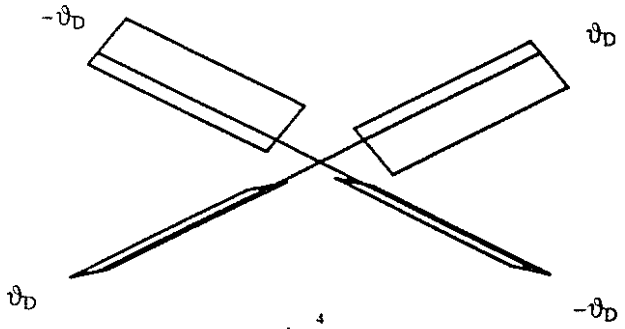

Figure 4d: Differential multiblade coordinate for a four-bladed rotor

This kind of separation leads to a block oriented structure of the controller as demonstrated in Fig. 5. The architecture allows to handle complex control tasks by dividing them in sub-tasks.

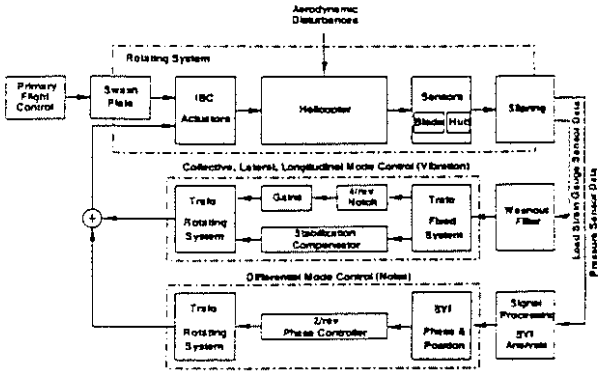

Figure 5: Controller architecture for simultaneous control of vibration and BVI noise

2.3. Noise Control

According to the results of the NASA Ames wind tunnel tests [4] several control principles and their mechanisms for the reduction of BVI noise for descendent flight conditions are discussed. As the interaction of a blade tip vortex to the rotor blade is identified as noise source, concepts which decrease the influence of the vortex are taken into consideration. Main parameters are the vortex strength at the formation location and the distance of the vortex passing the blade.

The approach is coincident with measurements showing minimum BVI noise for two azimuth positions where the first minimum of multicyclic pitch input is related to the locations of vortex formation and interaction, see Fig. 6. The functionality of the BVI noise reduction does not depend on a special harmonic although 2/rev blade pitch input offers the advantage of low amplitudes [2]. For the BO105 main rotor a higher harmonic blade pitch amplitude of approximately 1° proves to be sufficient for significant BVI noise reduction. The appropriate phase value depends on flight conditions. Improper control inputs lead to increased BVI noise.

The lack of an appropriate plant model makes the noise controller design difficult. Furthermore, the question of on board sensor systems arises as the objective aims on the reduction of the far noise field. Therefore, open loop flight tests were performed serving as data base for BVI noise controller development [5].

BVI noise control is split into two stages. The first stage consists in the detection of BVI noise as BVI noise obviously appears only under certain flight conditions. Blade mounted pressure transducers and microphones fixed at the landing gear supply data for BVI detection. In case of occurrence a 2/rev control has to be defined by amplitude and phase values. The 2/rev amplitude may be fixed to 1° blade pitch according to the results of the wind tunnel tests whereas the determination of the phase values depends on the selected controller design.

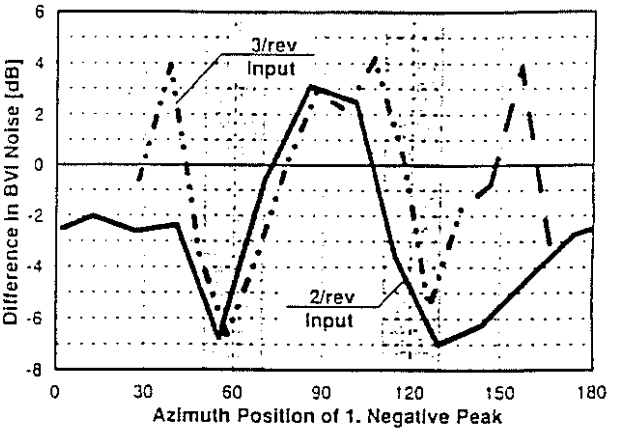

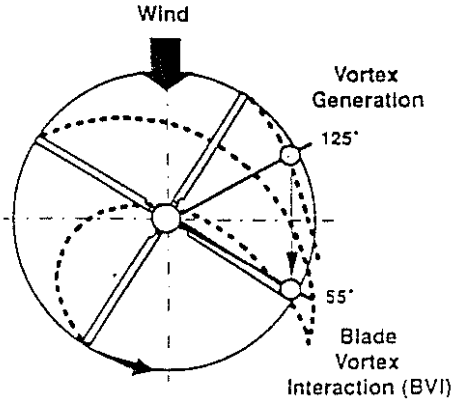

Figure 6: Powered descent condition with IBC inputs, (NASA Ames wind tunnel results)

A variety of controller concepts is discussed for BVI noise control differing in the choice of sensors and the kind of processing data. A more complex approach is

suggested by Deutsches Zentrum für Luft- und Raumfahrt (DLR) including an on-line identification algorithm into the controller.

In this report the controller design is concentrated on the vibration reduction part.

2.4. Vibration Control

Regarding vibration reduction the flight test campaign of 1990 and 1991 demonstrated that a significant change in cabin vibrations could be achieved for level flight at cruising speed [1], Fig. 7. The investigations of the flight test campaign were focused on single harmonic pitch input of 3/rev, 4/rev and 5/rev for vibration reduction purpose. The multicyclic pitch input leads to altered higher harmonic hub loads. If amplitude and phase values of the multicyclic pitch input are properly selected a cancellation of hub load components takes place.

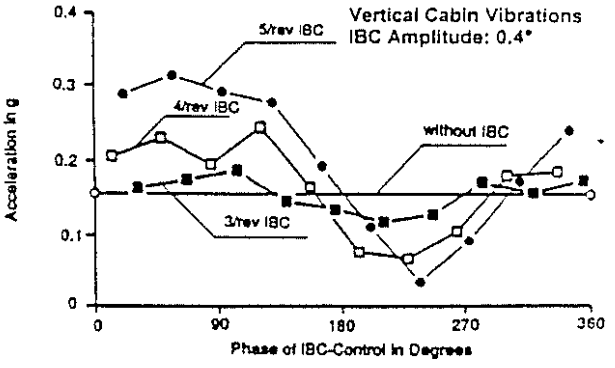

Figure 7: 4/rev vibration control by IBC (open loop) BO105 level flight tests 1991, μ=0.14

For the determination of the hub load changes due to multicyclic input, dynamic properties of the main rotor have to be taken into consideration. For the BO105 main rotor blades especially the first torsional eigenfrequency in the vicinity of 4/rev is of high importance for the dynamic behaviour. Fig. 8 shows the changes of 4/rev vertical hub forces due to higher harmonic input based on flight measurements and calculations.

The vibration controller regards undesired hub loads at blade passage frequency as disturbances to be eliminated. The task of the controller is the cancellation of these sinusoidal loads by exciting additional hub loads with appropriate amplitudes and opposite phase. Control theory calls this approach disturbance rejection. Due to the knowledge of the disturbance nature – sinusoidal at blade passage frequency – modern control theory offers special methods for controller design e.g. the implementation of servo-compensators [6]. Fig. 9.

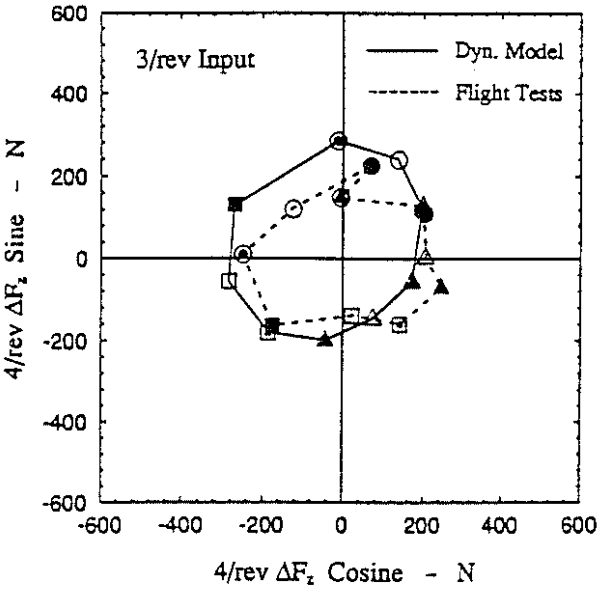

Figure 8a: 4/rev vertical hub force change due to 3/rev IBC input (nominal amplitude 0.4°)

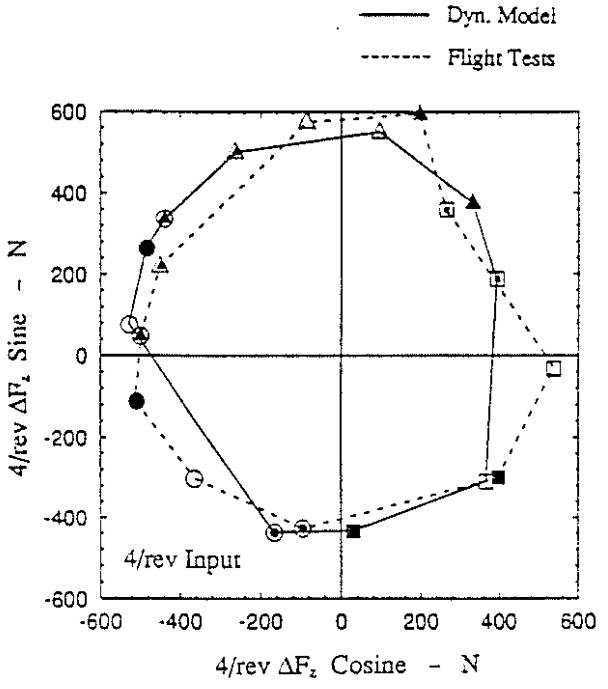

Figure 8b: 4/rev vertical hub force change due to 4/rev IBC input (nominal amplitude 0.4°)

2.5. Frequency Domain and Time Domain Concepts

Due to the periodicity of the excitations a conventional approach for vibration control is based on a Fourier analysis of the disturbances in order to derive a periodic control input by Fourier synthesis. The application of Fourier transformations leads directly to a frequency domain concept relating Fourier coefficients of the disturbances to Fourier coefficients of the

multicyclic blade pitch input. A transfer matrix T expresses the relationship between input and output assuming a quasisteady behaviour of the helicopter.

$$z = z_0 + T\Delta\theta$$

z	controlled output (Fourier coefficients)
z_0	uncontrolled disturbances (Fourier coefficients)
T	transfer matrix
$\Delta\theta$	control input (Fourier coefficients)

This relationship allows the calculation of control inputs eliminating or minimizing disturbances. The applicability of frequency domain vibration controllers is demonstrated by several institutions [7],[8].

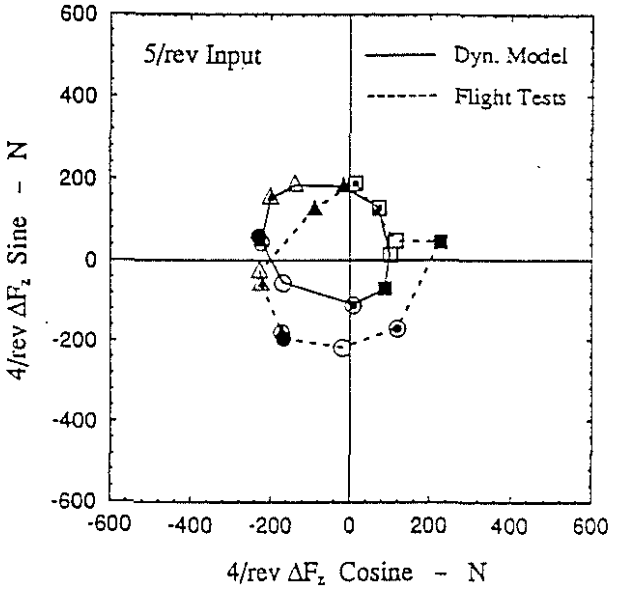

Figure 8c: 4/rev vertical hub force change due to 5/rev IBC input (nominal amplitude 0.4°)

Regarding sampling of the disturbance data for the Fourier analysis, information of at least one rotor revolution is required from theoretical point of view leading to a certain time delay for control. Furthermore, the assumption of quasisteady behaviour requires a dying out of the rotor transient response after updating the input. Therefore, the time delay has to be extended. Hall et.al. [9] showed that the time delay of conventional frequency domain concepts corresponds to low gain controllers. Low gains may cause an insufficient behaviour during transient manoeuvres and with respect to random disturbances.

Due to its basic simplicity, research teams has been interested in frequency domain concepts already in an early stage of multicyclic control development. An overview of several aspects concerning frequency domain vibration control is given in [10]. In addition Chopra et.al. [11] discussed numerical results of open and closed loop systems with and without identification showing possible sources of instability for some configurations.

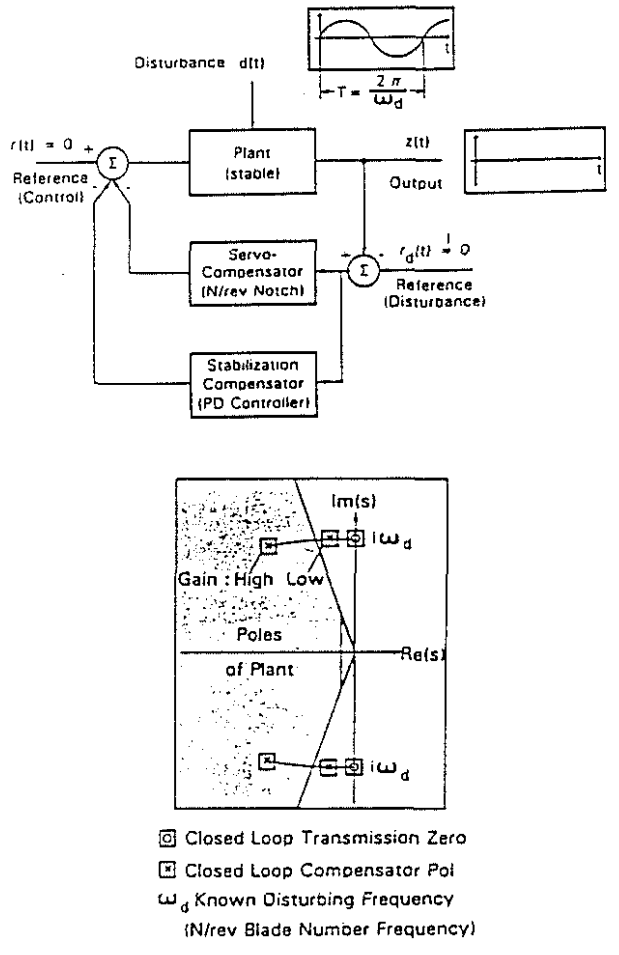

Figure 9: Disturbance rejection by output feedback control

On the other hand time domain controllers process time history information avoiding Fourier operations. Therefore, time domain controllers overcome the restriction of quasisteady behaviour as dynamic effects are implicitly considered. Concerning advanced controller designs, modern control theory focuses on time domain concepts based on linear time-invariant systems. The challenge is now to benefit from the perceptions of modern control theory for the helicopter vibration task.

In order to make a popular time-domain approach suitable for helicopter vibration control Gupta [12] suggests the modification of a linear-quadratic Gaussian (LQG) design procedure by the inclusion of frequency-shaped cost functionals tuned to the blade passage frequency. Hall et. al. [9] demonstrated some interesting similarities regarding the frequency domain approach and the time domain approach with respect to the narrow band disturbance rejection of classical

control theory. Furthermore, the role of the gain is discussed for a single input single output (SISO) system. The consideration of random disturbances leads to the demand for "high" gains obviously favouring time domain approaches.

The classical LQG design as well as other modern control concepts supposes a linear time-invariant (LTI) system. Under theoretical aspects the helicopter vibration problem in forward flight poses a linear time-periodic (LTP) problem due to the periodic conditions at the rotor blades. In order to consider the periodicity for controller design, procedures for optimal output feedback are worked out especially adapted to time periodic systems [13].

Linear time-periodic (LTP) system:

$$\dot{x}(t) = A(t)\,x(t) + B(t)\,u(t)$$
$$y(t) = C(t)\,x(t) + D(t)\,u(t)$$

x: state vector
u: input vector
y: output vector
t: time
A,...,D: time-periodic matrices

In order to reduce the LTP system into an adequate LTI system the matrices of the state space system are averaged in time. Before averaging the state space system is transformed into multiblade coordinates (MBC) improving the quality of the LTI system [14]. *The quality of the constant coefficient approach* increases with the number of blades and with decreasing advance ratio.

Linear time-invariant (LTI) system:

$$\dot{x}(t) = A\,x(t) + B\,u(t)$$
$$y(t) = C\,x(t) + D\,u(t)$$

A,...,D: constant matrices

Beside the vibration control task, the time domain concept permits the transfer of other solutions of modern control theory for control tasks. An important topic for helicopter rotors consists in the modification of the *system dynamics by feedback stabilization*. The skilful use of augmented modal damping leads to stabilized ground and air resonance conditions or improved response characteristics.

One goal of the RACT programme is to point out the benefits of time domain controller for active rotor control. The vibration control task is selected for several reasons. On the one hand the vibration control is of major importance for comfort improving the acceptance for passengers. On the other hand flight tests will directly demonstrate the applicability of this kind of controller.

3. Modern Control Theory Applied for Vibration Reduction

3.1. Output Feedback

The vibration control task consists of the elimination of a load vector (hub forces and moments at blade passage frequency) due to an input vector (multicyclic blade pitch inputs) defining a multiple input-multiple output (MIMO) system in terms of control theory. For the dynamics of MIMO systems the classical way of description is the usage of state space equations.

A typical representative for this approach is the linear quadratic Gaussian (LQG) regulator basing on state feedback. As the corresponding states of a helicopter responsible for vibrations are not directly measured – a problem occurring at the majority of control problems - control theory looked for alternative approaches. A straight forward way is the estimation of non-measurable states by state reconstructing leading to a more complicated controller design.

An alternative way is the direct feedback of output values eliminating the needs to know the states of the dynamic system [15]. An algorithm for the evaluation of optimal output feedback gains for a LTI system is given in [16] whereas Calise et.al. [13] focus on LTP systems. For the vibration control task an output feedback approach is selected as basic layout.

For control system design the dynamic system representing the helicopter is usually set up by the following time-variant linear system of equations whose state vector x, control vector u, disturbance vector d and output vector y are related by the following state space equations:

$$\dot{x}(t) = A(t)\,x(t) + B(t)\,u(t) + E(t)\,d(t)$$
$$y(t) = C(t)\,x(t) + D(t)\,u(t) + F(t)\,d(t)$$

A,...,F: time-periodic matrices

This equation system is based on the presumption of small perturbations due to the linearization of the generally non-linear helicopter behaviour. For steady flight conditions the defining matrices are periodic with respect to the main rotor azimuth angle (tail rotor periodicity is neglected). Further simplifications are now introduced by averaging the system matrices to constant matrices. The disturbances are introduced by explicit disturbance values d.

$$\dot{x}(t) = A\,x(t) + B\,u(t)$$
$$y(t) = C\,x(t) + D\,u(t) + I\,d(t)\,.$$

A,...,D: constant matrices
I: unity matrices

In its simplest form the output feedback is introduced by relating the output y to the input u by a constant feedback gain matrix:

$$u(t) = -K_C\, y(t)$$

K_C: feedback gain matrix

In a more general form the feedback loop includes additional dynamic components e.g. servo-compensators [6]. For the vibration controller Fig. 10 shows the basic output feedback loop consisting of:

- Plant
- Disturbance vector
- Servo-compensator block
- Feedback gain matrix
- Filter block (Wash-out)

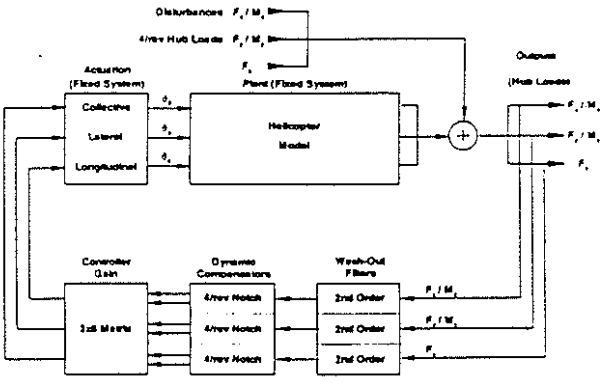

Figure 10: Basic components of hub load feedback loop for vibration control

The plant is partitioned into two dynamic systems modelling the actuators separately from the helicopter. The plant is excited by disturbances consisting of hub loads at blade passage frequency. The design goal is to eliminate these hub load components by output feedback.

For the elimination of the disturbances servo-compensators play an important role as discussed in chapter 3.3. Additional filters – e.g. wash-out filters – are also implemented in order to avoid adverse effects on primary flight control. A gain matrix appended to the servo-compensator block offers the possibility to adjust the properties of the vibration controller. The determination of this gain matrix is the key point for the functionality of the controller.

The state space system is defined in multiblade coordinates in order to improve the constant coefficient approximations. Therefore, the feedback loop determines the blade pitch inputs defined in the fixed system. The blade pitch vector consists of the collective control mode as well as the lateral and longitudinal control modes. The vibration controller has three degrees of freedom to its disposal for fulfilling the control task.

For a straight forward approach of the disturbance rejection principle, the number of control degrees of freedom equals the number of disturbances to be eliminated. Consequently, the hub load vector for control is limited to three elements. The controller affects also the remaining hub load elements in advantageous or disadvantageous sense depending on the plant properties. For simulation purposes two cases are selected, the elimination of the hub force vector (F_x, F_y, F_z) and the elimination of the vertical hub force, roll moment and pitch moment (F_z, M_x, M_y), in this paper described as hub load vector.

3.2. Plant Model

3.2.1. Helicopter Model

For the evaluation of the linearized state space system the comprehensive rotor code CAMRAD II is applied. CAMRAD II [17] offers two procedures for state space systems, the application of Floquet theory accounting for periodic systems and the performance of a constant coefficient approach approximating time variance by application of multiblade coordinates [10]. For the controller design the constant coefficient approach is selected.

The state space model of the BO105 is calculated in a two stage procedure of CAMRAD II. In a first step of the analysis the model has to be trimmed to a given flight condition. In order to represent a typical cruise flight condition the controller design is focused on level flight at 110 KTAS. Then, the state space system is set up by a linearization of the system equations using the trim solution as pivot point.

The helicopter model implemented for the vibration control purposes consists of two main components, the main rotor and the airframe including tail rotor. Finite element beams build the backbone of the elastic main rotor structure. Applying modal techniques seven blade modes (first and second lead-lag mode, first to fourth flap mode, first torsion mode) are considered for the main rotor. Using multiblade coordinates, the blade modes are transformed to rotor modes resulting in a frequency shift of $\pm$ 1/rev of the eigenvalues for the cyclic modes. The collective and differential modes are not affected (drive train modes are neglected).

Up to now the fuselage of the BO105 is implemented as rigid body introducing the inertial characteristics of the helicopter into the analysis. The implementation of an elastic airframe will follow. Aerodynamic effects of the fuselage and the stabilizer are considered by table data whereas the tail rotor is treated as a rigid rotor without degrees of freedom. For comparison two configurations of the helicopter model are used for deriving the state space system, a free flight configuration and a configuration with fixed rotor hub.

The free flight configuration includes rigid airframe degrees of freedoms representing the motion of the helicopter centre of gravity. Therefore, flight mechanical modes are part of the system leading to slightly unstable poles (phygoid). Controller optimizing algorithms often require a stable systems as starting point for the optimization procedure. In order to avoid unstable modes the rigid body degrees of freedom are eliminated fixing the rotor in space. The corresponding state space system is described as baseline case.

In order to model a dynamic system of the plant by CAMRAD II a first order state space system consisting of the four time-invariant matrices A, B. C and D was numerically evaluated. The dynamic behaviour of the plant obtained by CAMRAD II is described by the following equations:

$$\dot{x}(t) = A\,x(t) + B\,u(t)$$
$$y(t) = C\,x(t) + D\,u(t) + I\,d(t)$$

The disturbance of the dynamic system is considered by a disturbance vector d obtained by the CAMRAD II trim (The unity matrix I is introduced for matrix notation).

Validation of the state space system is a critical point especially due to appropriate data. For validation purposes comparisons are made referring results of CAMRAD II to data of the flight test campaign 1991. Fig. 8 shows the variation of the vertical hub force at blade passage frequency due to multicyclic input for several test points which differ in input phase. The flight conditions represent typical cruise flight at 110 KIAS.

3.2.2. Actuator Model

The actuators link the swashplate movements to the pitch horns introducing blade pitch to the rotor blades. For primary flight control the role of the actuators is identical to conventional pitch links. For IBC this arrangement allow to affect each blade individually by extension or contraction of the corresponding actuator.

In the frequency range of interest the actuators show a dynamic behaviour in experiments which has to be considered for controller design, see Fig. 11. The dynamic model of the IBC actuators bases on measurements of amplitude and phase values at different frequencies under unloaded and loaded condition. Theoretical work on the dynamic modelling of the actuator behaviour concluded that a transfer function of third order allows a good description of the actuator in the critical frequency range. Nevertheless, first or second order approximations are used for controller design in order to trade numerical stability of the design algorithms against accuracy.

3.2.3. Sensor System

The sensor system for the vibration controller consists of DMS sets for rotor shaft moments and blade bending moments. Accelerometers are mounted at several locations of the airframe. The hub loads required for output feedback are calculated by the available shaft and blade bending moments.

Concerning the shaft bending moments eight DMS sets are attached to the rotor shaft at two different planes. The DMS allow the measurement of four shaft bending moments, i.e. two perpendicular moments for every plane.

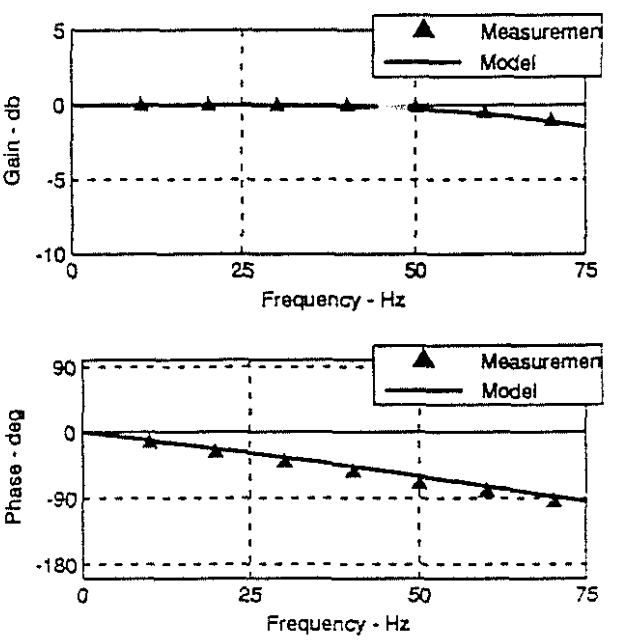

Figure 11: Dynamic behaviour of IBC blade root actuator

On every rotor blade two pairs of DMS sets are applied in order to measure blade flap moment and blade lead-lag moment. The DMS sets are located in the blade neck area. Hub forces and moments are estimated by extrapolation of the blade moments.

For modelling purposes hub forces and moments are directly selected as output variables. Concerning the hardware it has to be kept in mind that – contrary to the model – additional uncertainties are inherent in the determination of the hub loads by extrapolation.

3.3 Role of Servo-compensators

Ham [18] discussed and tested time domain controllers for active rotor control applications. The suggested system controls blade lag, flapping and bending dynamics leading to a modal control concept.

A more direct way for vibration reduction is the cancellation of disturbances by controlled excitations of corresponding magnitude and opposite phase values. In classical control theory this concept is known as disturbance rejection. An advanced way to handle disturbance rejection is the implementation of servo-compensators leading to robust control designs. According to Davison [6] a servo-compensator is a feedback compensator consisting of a number of sub-systems with identical dynamics depending on the nature of the disturbances.

The application of the "Internal Model Principle" implicitly considered in the servomechanism problem gives an instruction how to design the dynamics of the servo-compensator. In case of the vibration problem the disturbances are of sinusoidal nature at blade passage frequency. The "Internal Model Principle" postulates now a model of the disturbances which has to be included in the controller dynamics. Therefore, the sinusoidal behaviour of the disturbances is translated to undamped oscillators tuned to disturbance frequency.

The need for undamped oscillators in the feedback loop leads to the implementation of tuned notch filters. The notch filters are implemented in MATRIXx in state space form by the following equations:

$$A = \begin{bmatrix} 0 & 1 \\ -16\omega^2 & 0 \end{bmatrix}, \quad B = \begin{bmatrix} 0 \\ 1 \end{bmatrix},$$

$$C = \begin{bmatrix} 1 & 0 \\ 0 & 1 \end{bmatrix}, \quad D = \begin{bmatrix} 0 \\ 0 \end{bmatrix},$$

ω: main rotor angular velocity.

The notch filter has a pole pair located on the imaginary axis at a frequency of 4ω. According to the structure of the output matrix C both states of the notch filter are exported as output signals duplicating the number of signals. In Fig. 12 the dynamic behaviour of the notch filter is displayed. It is interesting to note that an approach of Gupta [12] using frequency-shaped cost functionals aims also at the usage of notch filters.

3.4. Gains and Stability

In order to study the servo-compensator concept theoretical investigations were made for the hover case where axisymmetric rotor conditions lead to a simplified rotor behaviour. The feedback of the vertical hub force acting on the collective input is selected for demonstration purposes in order to deal with a scalar value only.

Fig. 13 presents the block diagram of the feedback loop used for the disturbance rejection problem of the vertical hub force. The vertical hub force component is fed into the notch filter. The notch filter duplicates the feedback signal into two branches supplying both states of the notch. Two gains (factored for didactic reasons) $K\,\bar{k}_1$ and $K\,\bar{k}_2$ process the signals of the branches before they are summed together. This arrangement corresponds to some kind to classical PD controllers. The filter included in the block structure is of highpass kind used for wash-out of all signal components which may affect the primary flight control system.

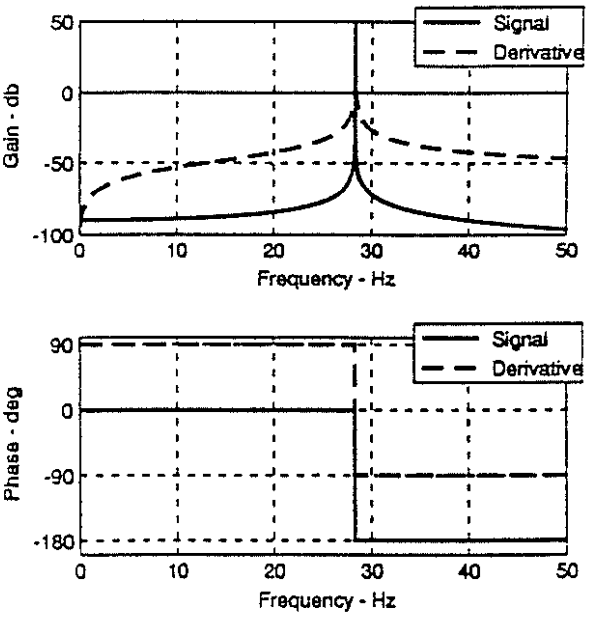

Figure 12: Dynamic behaviour of the notch filter, design frequency $4\omega = 28.3$ Hz

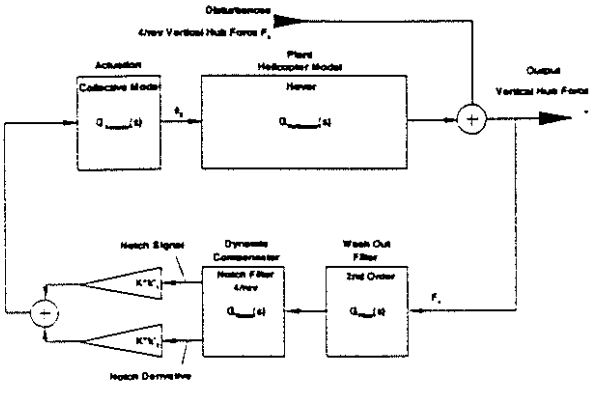

Figure 13: Vertical hub force feedback loop for hover

The closed loop transfer function of this system results in the following equation:

$$G(s) = \frac{z(s)}{d(s)} = \frac{1}{1 + (K\bar{k}_1 G_{No}(s) + K\bar{k}_2 G_{DNo/Dt}(s))\, G_{FAH}(s)}$$

using the abbreviation

$$G_{FAH} = G_{Filter}\ G_{Helicopter}\ G_{Actuator}\ .$$

z: output: controlled hub force component
d: disturbances: uncontrolled hub force component
$K\ \bar{k}_1$: signal gain
$K\ \bar{k}_2$: derivative gain
G_{No}: transfer functions notch signal
$G_{DNo/Dt}$: transfer function notch derivative
G_{FAH}: transfer function filter, actuator and helicopter block

At the blade passage frequency the transfer functions G_{No} and $G_{DNo/Dt}$ of the notch filter increase to infinity. From a physical point of view this behaviour is coincident with an undamped oscillator resulting in unbounded oscillations if excitations occur at resonance frequency. For the complete system (closed loop) the notch filters introduce the required transmission zeros for arbitrary gains $K\ \bar{k}_1$, $K\ \bar{k}_2$ (stability supposed). This concept is used for cancelling out sinusoidal disturbances at blade passage frequency.

$$G(i4\omega) = 0 \text{ (transmission zero)}$$

leading to disturbance cancellation

$$z(i4\omega) = G(i4\omega)\, d(i4\omega) = 0.$$

Therefore, the controller rejects any vertical hub force components acting at blade passage frequency for arbitrary $K\ \bar{k}_1$, $K\ \bar{k}_2 (\neq 0)$ in theory.

Nevertheless, the choice of the gains $K\ \bar{k}_1$, $K\ \bar{k}_2$ is restricted due to controller stability reasons. The determination of the gains is aimed on a favourable response behaviour under transient conditions. Numerical investigations show that the condition of closed loop stability limits the appropriate selection of the gains.

In order to study the influence of the gains to the controller behaviour, a vertical force at blade passage frequency is applied to the closed loop. In Fig. 15 a simple integral value representing the decay behaviour is chosen as ordinate. The evaluation of this value starts with the activation of the controller and stops 20 rotor revolutions later. The absolute area of the controlled output curve builds the ordinate value normalized by the disturbance curve, see Fig. 14.

A low level of q means a fast decaying response. Levels greater than one indicate instability of the closed loop system. As demonstrated in Fig. 15 only a finite interval of gain sets is appropriate with respect to stability. In order to interpret the mechanism of the gains $K\ \bar{k}_1$ and $K\ \bar{k}_2$ the transfer behaviour of the feedback is investigated for the case of a pure harmonic signal at blade passage frequency.

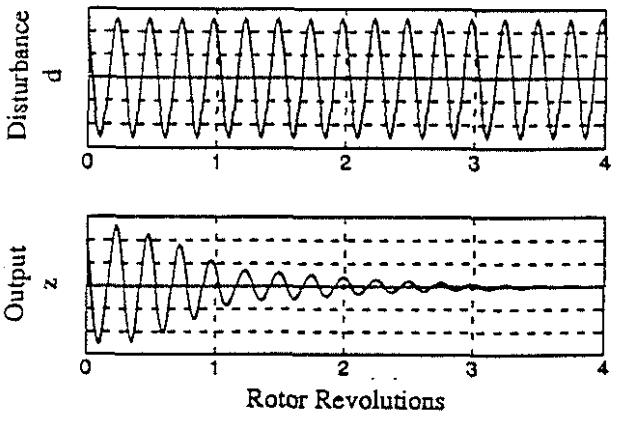

$$\text{Quality criterion transient response: } q = \frac{\int_{t_0}^{t_0+20T} |z(t)|\,dt}{\int_{t_0}^{t_0+20T} |d(t)|\,dt}$$

Figure 14: Definition of quality criterion for transient response

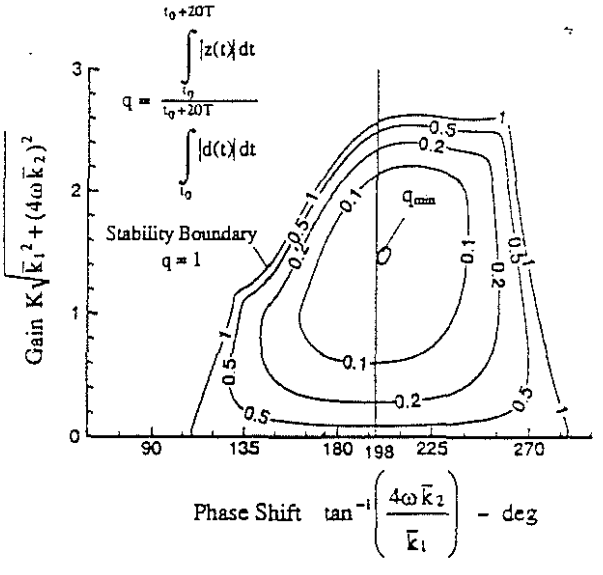

Figure 15: Stability and transient response of vertical hub force feedback for gains $K\ \bar{k}_1$, $K\ \bar{k}_2$

As the two notch filter states consist of a signal–signal derivative pair the states (outputs) of the notch filters are perpendicular for pure harmonic excitations. Vector diagrams are an appropriate tool for a geometrical interpretation of the gains. The vectorial linear combination of the two vectors due to the gains $K\ \bar{k}_1$ and $K\ \bar{k}_2$ offers the possibility to generate any desired amplification and phase shift of the incoming signal, see Fig. 16. The amplification and phase shift are given by the following formula:

Amplification $K\sqrt{\bar{k}_1^2+(4\omega\bar{k}_2)^2}$,

Phase (shift) $\tan^{-1}\left(\frac{4\omega\bar{k}_2}{\bar{k}_1}\right)$,

ω: main rotor angular velocity.

For disturbance rejection a vertical hub force component has to be generated by feedback with the same amplitude as the disturbance and opposite sign equivalent to a phase shift of 180°. As demonstrated above this condition will be fulfilled for every not vanishing combination of $K\,\bar{k}_1$ and $K\,\bar{k}_2$. In the following approach emphasis is given on the role of the phase shifts $\Delta\varphi_i$ for stability and transient response.

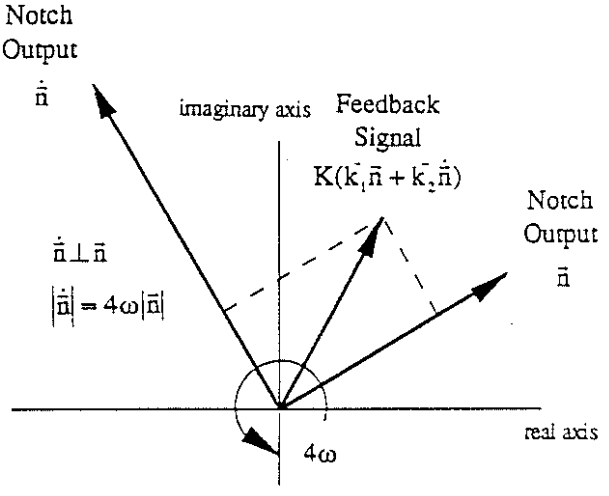

Figure 16: Composition of notch signals at blade passage frequency

The best transient response for the controller is expected for a total phase shift of 180° in the feedback loop as the feedback signal acts in phase opposition. For a signal at blade passage frequency, phase shifts of the components are calculated by the evaluation of the corresponding transfer functions with the Laplace variable set to $i4\omega$. Concerning the notch filter, perfect resonance conditions are assumed leading to a phase shift of -90° for the notch signal and a vanishing phase shift for the time derivative. Tuning the total phase shift of the feedback loop to 180° is achieved by special combinations of $K\,\bar{k}_1$ and $K\,\bar{k}_2$. The defining equation is:

$$\sum_i \Delta\varphi_i = 180°,$$

i = {notch filter, gain, filter, actuator, helicopter }
leading to

$$\Delta\varphi_{Gain} = 180° - (\Delta\varphi_{Notch} + \Delta\varphi_{Filter} + \Delta\varphi_{Act} + \Delta\varphi_{Heli})$$

For the components of the vertical feedback loop the sum of the phase shifts obtained at blade passage frequency amounts to

$$\Delta\varphi_{Notch} + \Delta\varphi_{Filter} + \Delta\varphi_{Act} + \Delta\varphi_{Heli} = -18.0°$$

The phase shift $\Delta\varphi_{Gain}$ depends on the gains $K\,\bar{k}_1$ and $K\,\bar{k}_2$ by the following formula:

$$\Delta\varphi_{Gain} = \tan^{-1}\left(\frac{4\omega\bar{k}_2}{\bar{k}_1}\right).$$

Combining these equations leads to a relationship between $\bar{k}_1$ and $\bar{k}_2$ demanding for a phase shift of 198°. In order to determine the gains additional conditions are required for the magnitude.

According to Fig. 15 gain sets which approximately fulfil a phase shift of 198° show preferable transient behaviour compared to other gain sets with same magnitude. Furthermore, phase shifts exist where no stability occurs. The extension of the stable area demonstrates a certain robustness of the controller with respect to magnitude and phase shift. These results may be used for a controller design procedure in combination with additional conditions dealing with stability considerations.

In order to increase the stability boundary towards higher gains work on extended controller concepts of the servomechanism problem is in progress, e.g. the generalized three-term controller [6].

For preparation of the general MIMO case this procedure is now translated to the usage of transfer functions. The total phase shift of −180° is expressed by the following formula based on the transfer function product of the components in the feedback loop:

$$\prod_i G_i = -K, \quad K \text{ real and positive}$$

i = {notch filter, gain, filter, actuator, helicopter }

The transfer function of the notch filter is unbounded at blade passage frequency. As only phase information is evaluated in the following steps the transfer function of the notch filter is replaced by the imaginary number -i and K is set to 1. Solving the product with respect to the gain leads to

$$G_{Gain} = (i\,G_{FAH})^{-1}$$

using the abbreviation

$$G_{FAH} = G_{Filter}\;G_{Helicopter}\;G_{Actuator}.$$

The real and imaginary part of the complex value G_{Gain} are rearranged leading to:

$$\bar{k}_1 = \text{real}(G_{Gain})$$

$$\bar{k}_2 = \text{imag}\left(\frac{G_{Gain}}{4\omega}\right).$$

The parameter K allows the adjustment of the controller with respect to stability and transient behaviour resulting in the final equations:

$$k_1 = K\,\bar{k}_1 = K\,\text{real}(G_{Gain})$$

$$k_2 = K\,\bar{k}_2 = K\,\text{imag}\left(\frac{G_{Gain}}{4\omega}\right).$$

3.5. A Design Procedure for a Decoupled Controller

The extension from the single input-single output (SISO) system of the last chapter to the complete *multiple input-multiple output (MIMO) system replaces* the two gain values k_1 and k_2 by a gain matrix connecting six inputs (from three notch filters) to three outputs (collective, longitudinal and lateral pitch input), see Fig. 10. The gain matrix has the following block structure:

$$K_C = \begin{bmatrix} \overbrace{k_{11}\ k_{12}}^{\text{Notch1}\ (n_1,\dot{n}_1)} & \overbrace{k_{13}\ k_{14}}^{\text{Notch2}\ (n_2,\dot{n}_2)} & \overbrace{k_{15}\ k_{16}}^{\text{Notch3}\ (n_3,\dot{n}_3)} & \} \text{collective} \\ k_{12}\ k_{22} & k_{23}\ k_{24} & k_{25}\ k_{26} & \} \text{longitudinal} \\ k_{13}\ k_{23} & k_{33}\ k_{34} & k_{35}\ k_{36} & \} \text{lateral} \end{bmatrix}$$

This paper presents two approaches for evaluating the gain matrix, a design procedure based on decoupling the MIMO system and a standard procedure of modern control theory.

The design procedure based on decoupling is derived straightforward from the results of the last chapter combined with a decoupling of the three feedback channels in order to build three systems of SISO kind. The equations of the SISO case changes from scalar to matrix form. The transfer functions G_i are now matrices, the corresponding signals vectors. In order to decouple the feedback channels, K is now defined as 3x3 real diagonal matrix with positive elements.

$$\prod_i G_i = -K, \quad K = \text{diag}(K_1, K_2, K_3)$$

i = {notch filter, gain, filter, actuator, helicopter}.

In accordance to the scalar case notch filters are considered by the matrix (-i I) and K is set to unity for the evaluation of the phase conditions.

The real and imaginary parts of the complex transfer function G_{Gain} have to be rearranged for the evaluation of a real gain matrix:

$$\bar{k}_{2i-1,j} = \text{real}\left(g_{ij}\right),$$

$$\bar{k}_{2i,j} = \text{imag}\left(\frac{g_{ij}}{4\omega}\right), \quad i=j=1,2,3.$$

Up to now the procedure bases only on criteria for decoupling and phase shift. According to the SISO case the elements K_1, K_2 and K_3 of the diagonal matrix K are used for an adjustment of the controller with respect to stability. Therefore, the elements of K_C are defined by the following equation:

$$K_C = \begin{bmatrix} K_1 & 0 & 0 \\ 0 & K_2 & 0 \\ 0 & 0 & K_3 \end{bmatrix} \begin{bmatrix} \bar{k}_{11}\ \bar{k}_{12} & \bar{k}_{13}\ \bar{k}_{14} & \bar{k}_{15}\ \bar{k}_{16} \\ \bar{k}_{21}\ \bar{k}_{22} & \bar{k}_{23}\ \bar{k}_{24} & \bar{k}_{25}\ \bar{k}_{26} \\ \bar{k}_{31}\ \bar{k}_{32} & \bar{k}_{33}\ \bar{k}_{34} & \bar{k}_{35}\ \bar{k}_{36} \end{bmatrix}$$

The decoupling offers the possibility to determine the magnitudes of the diagonal elements by the application of single input - single output (SISO) procedures accounting for stability for each feedback channel separately. This property is useful for experimental approaches e.g. defining the gain of each *feedback channel by manual adjustment.*

For decoupling, this approach needs only information of the dynamic system at blade passage frequency. Thus, results of flight tests allow an adaptation of the controller gain matrix with experimental results. This approach closes to some degree the gap between frequency and time domain although the controller bases on time domain concepts.

3.6. Optimal Output Feedback

The procedure for controller decoupling has assumptions and simplifications restricting the feasible performance of output feedback. The demand for decoupling of the feedback channels leads to a strong limitation for the gain matrix. Furthermore, stability is not implicitly considered. Therefore, methods of modern control theory are of interest for the evaluation of the gain matrix in a more advanced way.

The determination of the feedback gain matrix is equivalent to the optimal constant output feedback problem [13], [15] posed by the following equations. A linear time-invariant system is given by the following system of differential equations :

$$\dot{x}(t) = A\,x(t) + B\,u(t)$$
$$y(t) = C\,x(t) + D\,u(t)$$

In case of the vibration control task this state space system is the extended system including additional states of actuators and filters. As performance measure a standard infinite time quadratic performance criterion is defined

$$J = \frac{1}{2}\int_0^\infty [x'(t)\,Q\,x(t) + u'(t)\,R\,u(t)]\,dt$$

The matrices Q and R account for different units and weights of the state and input variables. Usually the matrices Q and R are selected as diagonal matrices. The choice of Q and R offers a possibility for the user to adjust the controller.

For output feedback the control u(t) is generated by output linear feedback with time-invariant feedback gains:

$$u(t) = -K_C\,y(t)$$

The determination of K_C is established by an optimization problem minimizing the performance criterion J. An iterative algorithm is described by Moerder et.al. [16]. The presented results are obtained by the application of the computer program MIMFOOF derived from [19].

3.7. Simulation Results

3.7.1. Suppression of Hub Loads: Baseline Case

The baseline case is defined by the following properties:

- configuration with fixed hub
- level flight 110 KTAS
- controller design by optimal output feedback
- no stabilization compensator
- simulation of continuous system

The dynamic properties of the helicopter model are represented by 56 states composed of seven modes for each blade. The state space system is defined in the fixed system. Therefore, components of the rotating system are transformed into multiblade coordinates, e.g. blade pitch input. Additional states referring to the actuators and to the filters exist.

In the baseline case the hub force vector (F_x, F_y, F_z) is used for output feedback. The input vector is defined in multiblade coordinates using the collective, the longitudinal and lateral control modes for vibration control. The inverse multiblade transformation relates these values to the pitch inputs of the individual blades.

Applying optimal output feedback theory, the controller depends on the appropriate choice of the diagonal matrices Q and R. For the presented cases the diagonal elements of Q are optimized with respect to the attenuation of the controlled hub forces. R is selected as unity. A non-linear iterative solution procedure leads to the elements of the gain matrix.

Fig. 17 presents a simulation of the baseline case showing a satisfying attenuation of the controlled hub forces in a few rotor revolutions after activation of the controller. Fig. 18 displays the eigenvalue solution of the closed loop system. The key point consists in the shift of undamped notch poles towards increased damping by feedback gains. The decay times of the controlled hub forces relate to the damping ratios of the notch filters.

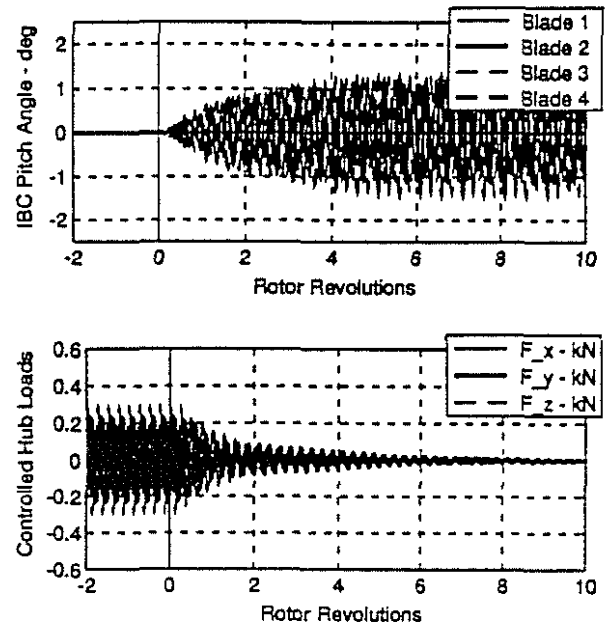

Figure 17: Suppression of 4/rev hub forces by IBC blade root actuation, level flight 110 kts (baseline case)

Furthermore, other pole locations alter by output feedback. The changes of the corresponding frequencies – defined by the ordinate values – are moderate concluding that the overall characteristics of the rotor are preserved.

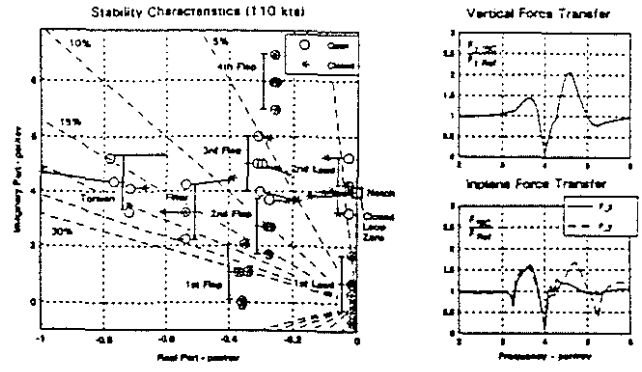

Figure 18: Analysis of 4/rev hub force disturbance rejection controller (baseline case)

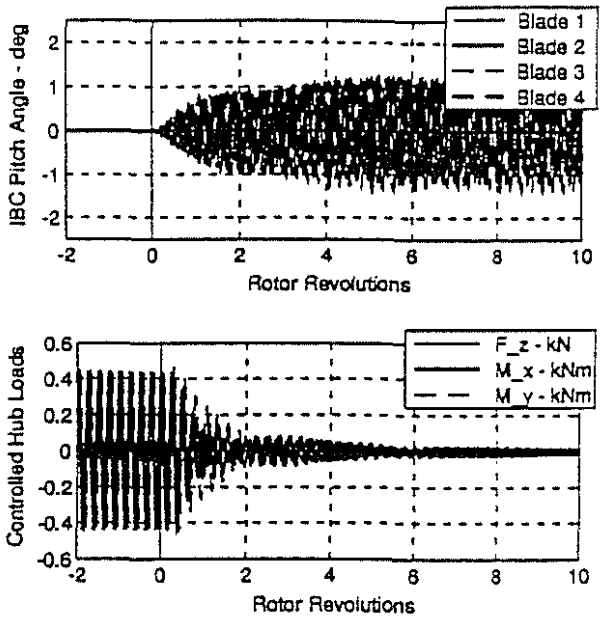

Figure 19: Suppression of 4/rev hub loads by IBC blade root actuation, level flight 110 kts

The functionality of the transmission zero is demonstrated in Fig. 18 comparing the controlled hub forces to the disturbances. Similar results yield for the feedback of hub roll and pitch moment components, see Fig. 19, Fig. 20.

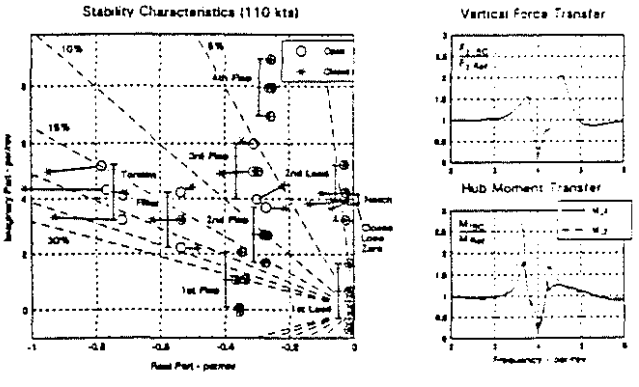

Figure 20: Analysis of 4/rev hub load disturbance rejection controller, level flight, 110 kts

For comparison the paper focuses now on the attenuation behaviour of the longitudinal hub force. In Fig. 21 the baseline controller and the decoupled controller show obviously similar performances although the procedures for calculating the gain matrices are quite different. For the decoupled controller optimization of the attenuation curves defines the missing scaling parameters.

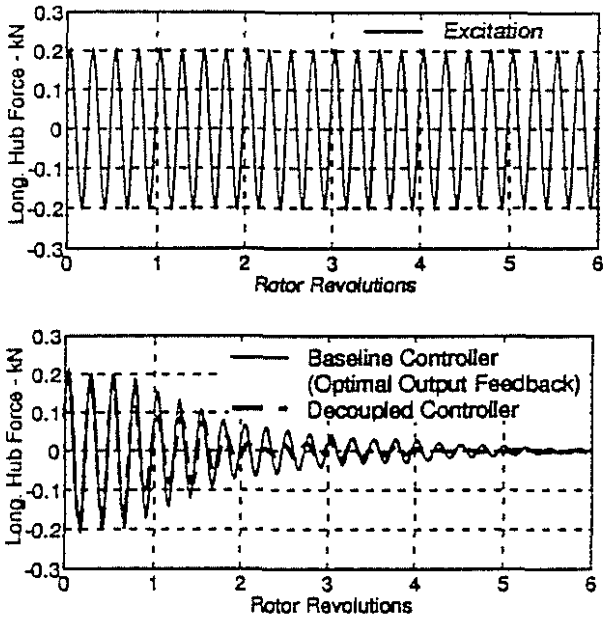

Figure 21: Comparison of optimal output feedback controller and decoupled controller

3.7.2. *Helicopter Model*

In a next step the complexity of the plant model is increased adding rigid body degrees of freedom to the baseline model. In this case the plant contains flight mechanical modes including the slightly unstable phygoid.

In Fig. 22 simulation results for the baseline controller applied to this plant model are presented. The inclusion of an elastic airframe is of interest for future work.

3.7.3. Controller Sensitivity to Flight Speed

The robustness of the vibration controller is a main topic due to the varying flight conditions affecting the dynamic properties of the helicopter. Simulations are performed with feedback gains designed for different flight speeds.

In Fig. 23 a gain matrix derived for the low speed transition regime (40 KTAS) is combined with a plant model representing a cruising flight speed of 110 KTAS. Fig. 23 demonstrates the ability of the controller to handle this mismatching condition with moderate performance degradation. No case of instability occurred for all investigated combinations of flight speeds ranging from 10 to 110 KTAS – obviously a consequence of the selected robust control concept. If some performance degradation is acceptable the vibration controller does obviously not require gain scheduling.

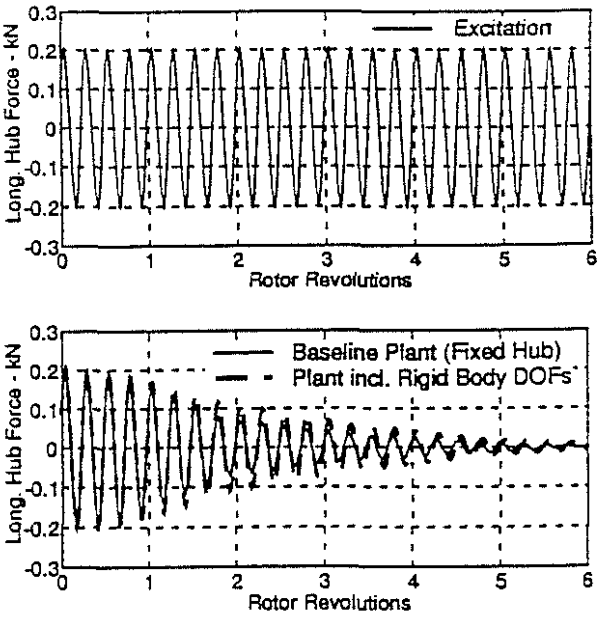

Figure 22: Comparison of baseline controller behaviour acting on different plants

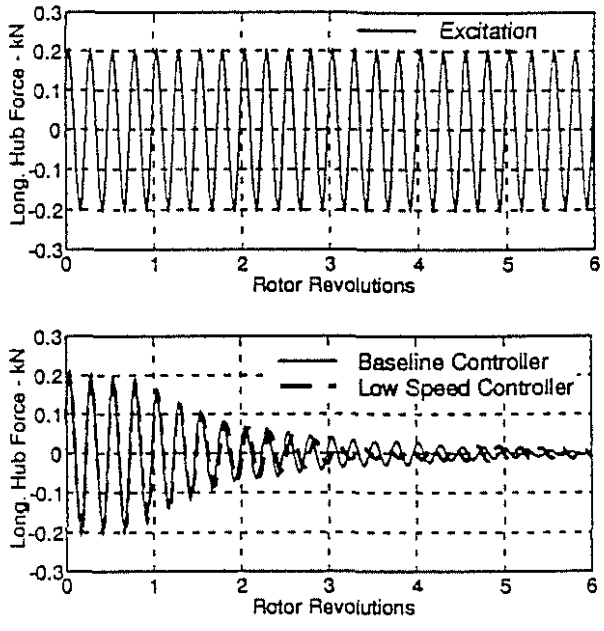

Figure 23: Comparison of baseline controller performances at different flight speeds (baseline 110 kts, low speed 40 kts)

3.8. Actual Aspects for Controller Design Development

The simulation results presented in the last chapter are very encouraging for planned applications on flight tests. Nevertheless, some fields are identified for improvements. First, the attenuation rates achieved by the decoupled controller as well as by optimal output feedback are obviously limited to similar levels. Increasing the gains significantly above the achieved level leads to unstable modes. Therefore, the benefit of higher gains can not be used without limitation. An approach for circumventing this limitation consists in the integration of additional stabilization compensators. Davison [6] suggested a general three term controller for the case of output feedback.

A more conceptual problem is seen in the disturbance rejection principle realized by the elimination of three outputs (hub loads) due to three rotor controls (collective, longitudinal, lateral control modes). Two different approaches are presented differing in the consideration of inplane hub forces or hub pitch and roll moments for output feedback. For hingeless rotor systems the elimination of hub forces could result in an increase of hub moments and vice versa depending on the plant properties.

As the simultaneous elimination of all load components is obviously not feasible by blade root actuated IBC, a minimization of these components is required. Mapping procedures are studied transforming the minimization approach into elimination conditions. As the transformation depends on flight states adaptive algorithms are envisaged.

4. Controller Realization and Implementation

4.1. Hardware Equipment of the Experimental Helicopter

The experimental IBC system is equipped with a rather complex hardware architecture in order to fulfil the challenging requirements for closed loop vibration and noise control. Two digital computers connected by transputer links build the core of the digital system: a system called 'IBIS' of the DLR Braunschweig and the digital computer on which the feedback controller is finally implemented. The 'IBIS' system is responsible for the processing and supply of sensor data. For digital systems in real-time operating conditions, characteristics as time steps and time delay are of major importance.

The core of the digital computer of the vibration controller is a Motorola 68060 processor. The infrastructure of the computer bases on the VME bus system. The sample rate of the real time application is adjusted to 64 times per cycle (nominal rotor frequency 7.07 Hz) sufficient for an appropriate Nyquist rate regarding vibration control. An angular encoder is used for synchronization of the computer clock to the rotor azimuth. The synchronization is used to tune the notch filters on-line to the actual rotor speed.

Tests of a prototype controller demonstrated that the performance of this computer fulfils real-time demands. The sample rate of the 'IBIS' system is higher in order to get a satisfying resolution for the pressure transducers used for BVI detection. The total time delay of the feedback controller is composed by the following items:

• Processing data and data transmission 'IBIS': The time used for processing sensor signals and transmitting data from 'IBIS' to the vibration control computer is approximated by 1ms.

• Processing Time: In order to calculate the required feedback control, the vibration control computer needs a finite time step. A time step of about 2 ms has to be taken into account according to the sampling rate.

• Zero Order Hold (ZOH): The blade root actuators are controlled by analogous signals. Therefore, digital-analogue converters (DAC) of the output board transform the digital signals operating in a zero order hold modus. This means that the output signals are kept constant during a time step. Improved concepts include the linear point connector (LPC).

The resolution of the sensor signals is limited to 12 bit, the resolution of the output boards amounts to 16 bit. Quantization effects due to the limited resolutions is a point of interest for future work.

4.2. Controller Realization

The progress of numerical tools supporting the design and implementation of feedback controllers on a high level leads to the development of program packages specialized for the design of control systems. These packages basically developed from matrix environments and block diagram tools are known under the designation Computer-aided Design (CAD) for control or more precisely Computer-aided Control System Design (CACSD) [20].

These tools support the designer in a wide range of different disciplines from simple matrix manipulations to transfer of the design into an embedded real-time controller code. The usage of such highly integrated packages is in coincidence with the ideas of rapid prototyping having advantages on the fields of flexibility, time and quality assurance compared to conventional methods. The design of the vibration controller is performed by the CACSD package MATRIXx [21]. Fig. 24 gives an overview with respect to the integration of the modules used for the design process.

The plant is obtained by combination of the aeromechanical state space model of the helicopter as result of CAMRAD II and the actuator model defined by a transfer function. Further algebraic components exist e.g. the multiblade and inverse multiblade transformations. The components are connected by assignment of inputs and outputs.

The controller is realized by the implementation of notch filters as servo-compensators and additional filters - e.g. wash-out filters. The assembly of plant and controller components is used as input data for the controller optimization procedures based on optimal output feedback [19] for the vibration controller. The implementation of other controller configurations – for instance H_∞ – is easily performed by the modular architecture of MATRIXx.

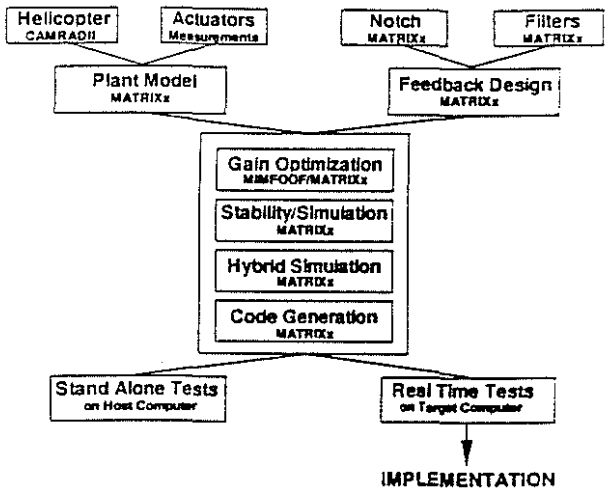

Figure 24: Flow chart of vibration controller development process using CACSD-tools

Next, the optimized gain is inserted into the block structure of the controller closing the loop of the feedback system. MATRIXx offers eigenvalue solvers for stability investigations of the closed loop system as well as time domain simulations revealing the transient behaviour of the controller. MATRIXx supports the user transforming the continuous system into discrete or hybrid form.

The code generation module leads to automatic coding of the isolated controller or the entire control system. Implementation and testing on the host is possible as well as cross-compiling for real-time evaluation and application on the target computer. The usage of templates allows customizing the generated code for the application.

Concluding the design procedure the controller development is an highly integrated process guaranteeing flexibility and fast development times as well as high quality due to the elimination of possible manual faults.

4.3. Discrete and Hybrid Systems

Time delay may play a disadvantage role for stability of closed loop systems. Therefore, the affection of time delay on closed loop performances is a point to be investigated. As the controller gain optimization is based on a continuous system, the digital hardware components are emulated with adequate time delays.

The transformation of a continuous block into discrete form is a typical task for the favourable

application of CACSD packages. MATRIXx offers several methods for the transformation procedures divided into numerical differentiation methods, Z-transform and pole-zero mapping. As indicated by the number of methods the mapping of a continuous system into a discrete system is not unique. All methods have disadvantages due to distortion.

For the vibration controller the preservation of the servo-compensator design frequency is unimpeachable. Therefore, special emphasis has to be given on the transformation method for the servo-compensator. Tustin's rule in combination with prewarping is a method preserving the blade passage frequency as design frequency. The following transformation is applied:

$$s = 2\pi f \cot(\pi f\, dt)\frac{z-1}{z+1},$$

s	Laplace variable (continuous)
f	blade passage frequency
dt	time step
z	z variable (discrete)

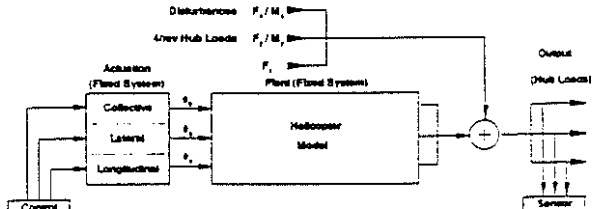

Figure 25: Block diagram of the vibration control feedback loop including digital systems

Fig. 26 presents a simulation of the hybrid system shown in Fig. 25 which is compared to the corresponding continuous system including time delays. No significant degradation is noticed confirming the applied transformation.

Fig. 27 presents the block diagram of the vibration controller with respect to physical sensor and control data. Therefore, multiblade transformations and their inverse counterparts have to be considered explicitly transforming data between the rotating and the fixed system.

4.4. Automatic Code Generation

For users the capability of an automatic generation of real-time code has already been of high interest in an early stage of the CACSD development. The development of code generators is still in progress emphasizing on optimization of execution speed and memory allocation.

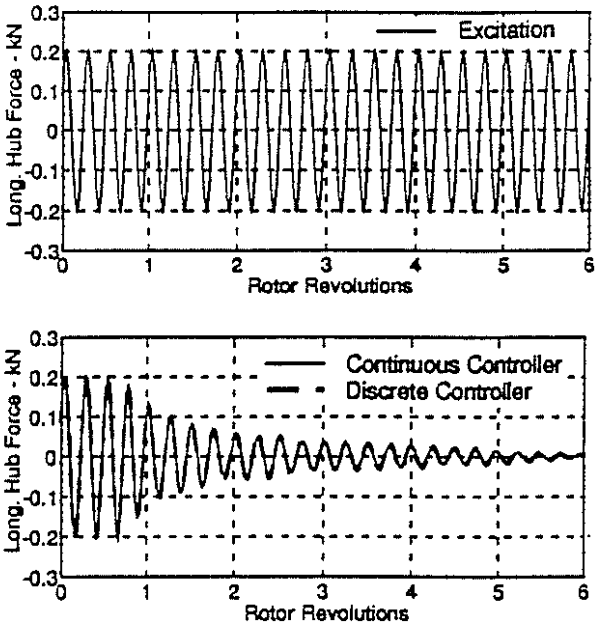

Figure 26: Comparison of the controller performance: continuous versus hybrid simulations

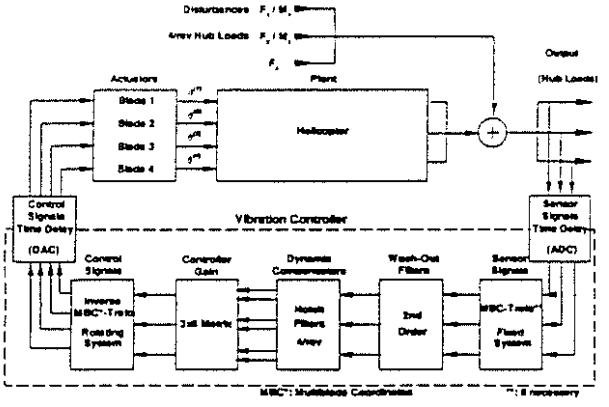

Figure 27: Block structure of the vibration control feedback loop including transformations between fixed and rotating system

The automatic code generation of MATRIXx is designed under the aspect of adaptivity in order to serve a variety of applications ranging from stand-alone simulations on the host up to real-time applications on the target. Therefore, MATRIXx uses template files for customization of the code generation.

For a real-time application a template program is typically composed by the following modules:

- Scheduler: The scheduler serves as frame of the real-time program. The scheduler is responsible for the performance of external input/output functions and for the dispatch list containing the tasks to be executed.

Further administrative tasks are assigned to the scheduler, too.

- Dispatcher: The dispatcher passes control to the task with the highest priority in the dispatch list.
- Sub-systems: The sub-systems or tasks build the core of the controller. Each control task is translated to a sub-system.
- Timer Interrupt Handler: The timer interrupt handler defines the time for the scheduler. For simulations on the host the timer interrupt handler is not needed.
- Input/Output Routines: Input/output routines are mainly used for the stand-alone mode (e.g. on the host) using external files for input and output.

The user has the possibility to tailor each of these modules to his specific needs.

4.5. Flap Actuation: A Case Study Using CACSD Tools

According to [22] and [23] the actively controlled flap offers advantages in the fields of power consumption and airworthiness. Therefore, the RACT programme embraces the development of a piezoelectric flap control unit in addition to the work on the conventional IBC system. This unit was developed by the Daimler-Benz Research and Technology Sector and recently tested in the transonic wind tunnel of the DLR in Göttingen [24].

For preliminary investigations of blade flap actuation the BO105 model is modified by additional flap definitions demonstrating the benefits of the highly integrated development system. The development tools presented in chapter 4.2. offer the possibility to repeat the controller design with minor changes. The modified actuation system affects the matrices B and D of the helicopter state space model. These matrices describe the connection between control and state vector in case of B and control and output vector in case of D. Actuator dynamics are neglected assuming an appropriate bandwidth of the flap actuators. The flap extends over 10% blade span and 15% blade chord.

Fig. 28 shows that the flap has the potential to reduce vibrations exhibiting a behaviour similar to those of conventional blade root actuated IBC systems. Further points of interest e.g. flap deflections, power consumption and pitch link loads have to be investigated.

5. Summary

For an actual research programme on the fields of multicyclic control this paper focuses on the vibration control task which is one of the key points for future improvements of helicopter technology. Two aspects are emphasized for the development of the vibration controller. First a time domain concept for the controller is presented relating this concept to modern control theory and comparing it to alternative approaches. The controller development aims on closed loop flight tests of a BO105 modified for IBC by blade root actuators.

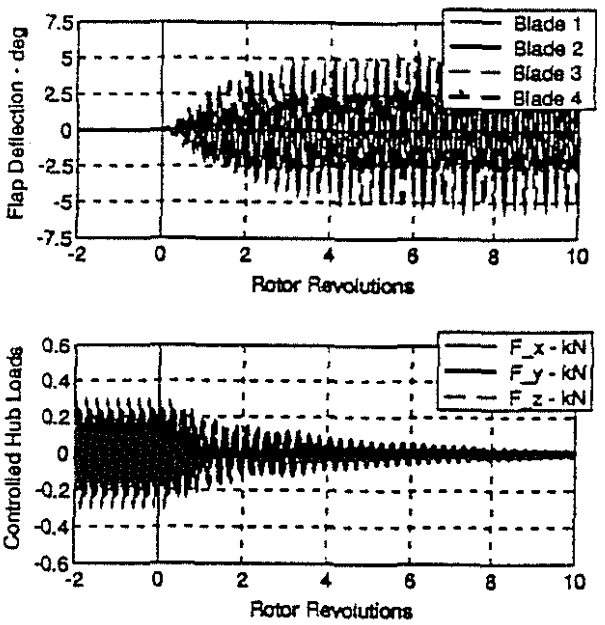

Figure 28: Suppression of 4/rev hub forces by blade flap actuation, level flight 110 kts

Beside these more theoretical considerations the paper lights the role of modern simulation tools under industrial points of view. The application of these tools starts with advanced modelling capabilities of the helicopter and ends with downloading of the real-time code automatically generated for the digital control system. The usage of integrated and automated procedures leads to a highly flexible controller development environment allowing investigations of alternative concepts (actuation, controller concepts, ...) in a minimum of time.

In order to underline the idea of flexibility in controller development and to give simultaneously an outlook for advanced actuation systems – a case study replacing the blade root actuation by an actively controlled flap – is discussed with respect to the controller design process.

References

[1] Teves, D., Klöppel V., Richter P.,"Development of Active Control Technology in the Rotating System, Flight Testing and Theoretical Investigations", 18th European Rotorcraft Forum, Avignon, France, 1992.

[2] Jacklin, S. A., Blaas A., Teves, D., Kube R., "Reduction of Helicopter BVI Noise, Vibration and Power Consumption Through Individual Blade Control", 51st Annual Forum of the American Helicopter Society, Fort Worth, 1995.

[3] Schimke, D., Jänker, P., Blaas, A., Kube, R., Schewe, G., Keßler, Ch.," Individual Blade Control by Servo-Flap and Blade Root Control: A Collaborative Research and Development Programme", 23rd European Rotorcraft Forum, Dresden, Germany, 1997.

[4] Niesl, G., Swanson, S.M., Kube, R. , Jacklin, S.A., Blaas, A.,"Effect of Individual Blade Control on Noise Radiation", AGARD Aeroacoustic Conference, Berlin, 1994.

[5] Schöll, E., Gembler W., Bebesel, M., Splettstößer W., Kube R., Pongratz, R.,"Noise Reduction by Blade Root Actuation - Analysis of Flight and Wind Tunnel Tests", 24th European Rotorcraft Forum, Marseilles, France, 1998.

[6] Davison E.J. and Ferguson, I.J.,"The Design of Controllers for the Multivariable Robust Servomechanism Problem Using Parameter Optimization Methods", IEEE Transactions on Automatic Control, Vol.AC-26, No.1, 1981.

[7] Wood, E.R., Powers, R.W., Cline J.H., Hammond, C.E.,"On Developing and Flight Testing a Higher Harmonic Control System", 39th Annual Forum of the American Helicopter Society, St.Louis, Missouri, 1983.

[8] Polychroniadis M., and Achache M.,"Higher Harmonic Control : Flight Tests of an Experimental System on SA 349 Research Gazelle", 42nd Annual Forum of the American Helicopter Society, Washington, 1986.

[9] Hall, S. and Werely, N.,"Linear Control Issues in the Higher Harmonic Control of Helicopter Vibrations", 45th Annual Forum of the American Helicopter Society, Boston, 1989.

[10] Johnson, W.,"Self-tuning Regulators for Multicyclic Control of Helicopter Vibration", NASA Technical Paper 1996, 1982.

[11] Chopra, I. and McCloud, J.L., III, "Considerations of Open-loop, Closed-loop and Adaptive Multicyclic Control Systems", American Helicopter Society Northeast Region National Specialists' Meeting on Helicopter Vibration, Hartford, Connecticut, 1981.

[12] Gupta, N.,"Frequency-shaped Cost Functionals: Extension of Linear-Quadratic-Gaussian Design Methods", AIAA, Vol.3,No.6,1980.

[13] Calise, A.J., Wasikowski, M.E., Schrage, D.P., "Optimal Output Feedback for Linear Time-periodic Systems", Journal of Guidance, Control and Dynamics, Vol.15, No.2, 1992.

[14] Johnson, W.,"Helicopter Theory", Princeton University Press, 1980.

[15] Levine, W.S. and Athans, M.,"On the Determination of the Optimal Constant Output Feedback Gains for Linear Multivariable Systems", IEEE Transactions in Automatic Control, Vol.AC-15, No.1, 1970.

[16] Moerder, D.D. and Calise A.J.,"Convergence of a Numerical Algorithm for Calculating Optimal Output Feedback Gains",IEEE Transactions on Automatic Control, Vol.AC-30, No.9, 1985.

[17] Johnson, W.,"CAMRAD II", Manuals, Johnson Aeronautics, 1997.

[18] Ham, N.D.,"Helicopter Gust Alleviation, Attitude Stabilization and Vibration Alleviation Using Individual-Blade-Control through a Conventional Swash Plate", 11th European Rotorcraft Forum, Paper No.75, 1985.

[19] Wasikowski, M.,"An Investigation of Helicopter Individual Blade Control Using Optimal Output Feedback", Thesis, Georgia Institute of Technology, 1989.

[20] Rimvall, C.M. and Jobling C.P.,"Computer-Aided Control Systems Design", Chapter 23 of The Control Handbook, edited by Levine, W.S., CRC Press, 1996.

[21] Floyd, M.A., Dawes, P.J., Milletti, U.," X-Math: A New Generation of Object-oriented CACSD Tools", Proceedings European Control Conference 3, 2232-2237, Grenoble, France, 1991.

[22] Friedmann, P.P. and Millott, T.A.,"Vibration Reduction in Rotorcraft Using Active Control: A Comparison of Various Approaches", Journal of Guidance, Control and Dynamics, Vol.18, No.4, July-August 1995.

[23] Milgram, J. and Chopra I.,"Dynamics of an Actively Controlled Plain Trailing Edge Flap System for a Modern Bearingless Rotor", 23rd European Rotorcraft Forum, Dresden, Germany, 1997.

[24] Schimke, D., Jänker, P., Wendt, V., Junker, B.,"Wind Tunnel Evaluation of a Full Scale Piezoelectric Flap Control Unit", 24th European Rotorcraft Forum, Marseilles, France, 1998.